Adaptive response of the murine collecting duct to alkali loading

Genini, Alessandro ; Mohebbi, Nilufar ; Daryadel, Arezoo ; Bettoni, Carla ; Wagner, Carsten A

Abstract: Fine-tuning of salt and acid-base homeostasis is achieved in the renal collecting duct through the action of intercalated and principal cells. Their activity is tightly regulated adapting to changes in systemic acid-base, fluid, or electrolyte status. The relative number of acid or bicarbonate secretory intercalated cells changes in response to acid or alkali loading. Several factors that may induce collecting duct plasticity in response to acid loading have been identified including cell proliferation, Growth Differentiation Factor 15 (Gdf15), hensin (DMBT1), and SDF1 (or CXCL12). Also, the transcription factors Foxi1 and CP2L1, or the Notch2-Jag1 signaling pathway, may play a role. However, little is known about the mechanisms mediating the adaptive response of the collecting duct to alkali loading. Here, we examined in mouse kidney the response of these factors to alkali loading. Mice were left untreated or received $NaHCO_3$ or NaCl over 7 days. Cell proliferation in vivo was monitored by Ki67 labeling or BrdU incorporation and expression of cell markers, and regulatory factors were examined. Foxi1 and GDF15 were upregulated and CP2L1 downregulated during alkali loading. Ki67 staining and BrdU incorporation were frequent in AQP2-positive cells in the NaCl and $NaHCO_3$ groups, but no evidence was found for increased Ki67 or BrdU staining in bicarbonate-secretory cells consistent with a model that AQP2 positive precursor cells may differentiate into intercalated cells. Thus, alkali loading alters the cellular profile of the collecting duct, which may involve cell proliferation and changes in the network of molecules determining the plasticity of the collecting duct.

DOI: https://doi.org/10.1007/s00424-020-02423-z

Adaptive response of the murine collecting duct to alkali loading

Alessandro Genini[1*], Nilufar Mohebbi[1,2*], Arezoo Daryadel[1], Carla Bettoni[1], Carsten A. Wagner[1]

[1]Institute of Physiology, Zurich, Switzerland, [2]Division of Nephrology, University Hospital Zurich, Zurich, Switzerland.

*A. Genini and N. Mohebbi contributed equally and therefore share first authorship

Corresponding author

Carsten A Wagner
Institute of Physiology
University of Zurich
Winterthurerstrasse 190
CH-8057 Zurich
Switzerland
Phone: +41-44-63 55023
Fax: +41-44-63 56814
Wagnerca@access.uzh.ch

Acknowledgments

The use of the ZIRP Rodent facility is gratefully acknowledged. The study was supported by grants from the Swiss National Science Foundation (31003A,155959 and 176125) to C. A. Wagner.

Disclosure

All authors report no conflict of interest

Authors contribution

A.G., N.M., A.D., C.B., and C.A.W. performed experiments and analyzed data, A.G., N.M. and C.A.W. wrote the manuscript, all authors read and approved the manuscript.

ABSTRACT

Fine-tuning of salt and acid-base homeostasis is achieved in the renal collecting duct through the action of intercalated and principal cells. Their activity is tightly regulated adapting to changes in systemic acid-base, fluid or electrolyte status. The relative number of acid or bicarbonate secretory intercalated cells changes in response to acid- or alkali-loading. Several factors that may induce collecting duct plasticity in response to acid-loading have been identified including cell proliferation, Growth Differentiation Factor 15 (Gdf15), hensin (DMBT1), and SDF1 (or CXCL12). Also the transcription factors Foxi1 and CP2L1, or the Notch2-Jag1 signaling pathway may play a role. However, little is known about the mechanisms mediating the adaptive response of the collecting duct to alkali loading. Here we examined in mouse kidney the response of these factors to alkali-loading. Mice were left untreated or received $NaHCO_3$ or NaCl over 7 days. Cell proliferation *in vivo* was monitored by Ki67 labeling or BrdU incorporation and expression of cell markers and regulatory factors were examined. Foxi1 and GDF15 were upregulated and CP2L1 downregulated during alkali loading. Ki67 staining and BrdU incorporation were frequent in AQP2-positive cells in the NaCl and $NaHCO_3$ groups but no evidence was found for increased Ki67 or BrdU staining in bicarbonate-secretory cells consistent with a model that AQP2 positive precursor cells may differentiate into intercalated cells. Thus, alkali loading alters the cellular profile of the collecting duct, which may involve cell proliferation and changes in the network of molecules determining the plasticity of the collecting duct.

Key words: Alkalosis, kidney, collecting duct, pendrin, remodeling, intercalated cell differentiation

INTRODUCTION

The renal collecting duct adapts to the systemic acid-base status by excreting either acids or alkali [54]. The epithelium of the collecting duct consists of two major cell types, segment specific principal cells and intercalated cells [11,39]. Principal cells serve mainly the reabsorption of sodium through the epithelial sodium channel (ENaC), water through the water channels AQP2 and AQP3, and the secretion of potassium through ROMK channels [28]. Acid-secretory intercalated cells express the chloride/bicarbonate exchanger anion exchanger 1 (AE1, SLC4A1) at their basolateral side and vacuolar-type H^+-ATPases (V-type H^+-ATPases) at their luminal pole [11,4]. In contrast, alkali-secretory type B intercalated cells are characterized by the presence of the chloride/bicarbonate exchanger pendrin (SLC26A4) at the apical membrane and V-type H^+-ATPases at the basolateral side [11,40,57]. Another type of intercalated cells may exist, non-A/non-B-intercalated cells expressing luminal pendrin and V-type H^+-ATPases at their luminal (and basolateral) membrane [47,26]. Intercalated cells expressing pendrin may serve not only the secretion of bicarbonate but may also be important for sodium chloride balance and hence blood pressure control. Pendrin functions in concert with the Na+-driven chloride-bicarbonate exchanger NDBCE to mediate chloride reabsorption. This activity is regulated by NaCl depletion, aldosterone and angiotensin and required to maintain blood pressure during NaCl depletion or if overactivate to cause hypertension in animal models [44,24,17,19,27,58,61,50,60]

The relative abundance and activity of all these cell types varies with changes in electrolyte and acid-base status and is, at least in part, regulated by several hormones and factors that link volume and acid-base control [54]. Acidosis increases the activity and the relative abundance of type A intercalated cells whereas alkalosis stimulates type B intercalated cells and enhances their relative abundance [54]. Several factors and signaling cascades have been identified that are involved in the plasticity of the collecting duct system in response to an acid-load. These factors include the Growth Differentiation Factor 15 (GDF15) [12], hensin (also known as DMBT1) and integrins [16,3], stromal cell-derived factor 1 (SDF1, also known as CXC-Motif-chemokine 12 (CXCL12) or pre-B cell growth-stimulating factor (PBSF)) [43], Adam10 [18], and Notch1 and 2 together with JAG2 [46], that alone or together may induce interconversion of cells (e.g. from principal to intercalated cells or from type A to type B intercalated cells) and/or cell proliferation of specific cell types [12,63]. In addition, several factors may be critical for the developmental organization of the collecting duct and

differentiation of cell types such as Foxi1 or the grainyhead-related transcription factor, CP2-like 1 (CP2L1) [68,34,66] or p53 [13]**.** Cell fate tracing experiments as well as deletion of factors involved in maintaining principal cell properties suggest that AQP2 expressing cells can serve as precursors for both type A and type B intercalated cells [49,67,18]. Similarly, some cells from the distal convoluted tubule expressing the thiazide-sensitive NaCl cotransporter (NCC) may also differentiate into type B intercalated cells [49].

In contrast to acidosis, little is known about the adaption of the collecting system to alkali loading. Alkalosis reduces proton secretion by type A intercalated cells and stimulates bicarbonate secretion along the connecting tubule and cortical collecting duct [15,51]. Moreover, recovery from acidosis or induction of alkalosis are associated with a reduction in the relative abundance of type A intercalated cells and a relative increase in type B intercalated cells. However, the mechanisms underlying this adaptive response have not been characterized. Here, we induced alkalosis by oral loading of mice with $NaHCO_3$. Two groups of mice served as controls, untreated mice and mice receiving equimolar amounts of NaCl in their drinking water to account for the effects of sodium loading. Our results demonstrate that chronic but not acute $NaHCO_3$ loading increased the relative frequency of pendrin positive type B intercalated cells in the connecting tubule, stimulated a transient increase of pendrin mRNA and protein after 24 hrs, and was associated with changes in several factors involved in collecting duct patterning.

MATERIALS AND METHODS

Animal Experiments

Male C57BL/6J mice (Harlan, Germany), 12 weeks old, were randomly assigned to different 12 groups: 1) no treatment (control) for 12 hours, 2) no treatment (control) for 24 hours, 3) no treatment (control) for 2 days, 4) no treatment (control) for 7 days, 5) 0.28 mol/L NaCl in drinking water for 12 hours, 6) 0.28 mol/L NaCl in drinking water for 24 hours, 7) 0.28 mol/L NaCl in the drinking water for 2 days, 8) 0.28 mol/L NaCl in drinking water for 7 days, 9) 0.28 mol/L $NaHCO_3$ in drinking water for 12 hours, 10) 0.28 mol/L $NaHCO_3$ in drinking water for 24 hours, 11) 0.28 mol/L $NaHCO_3$ in drinking water for 2 days, and 12) 0.28 mol/L $NaHCO_3$ in drinking water for 7 days (n = 5-10 per group). To study cell proliferation in vivo, some animals were injected intraperitoneally with 5-Bromo-2´-deoxyuridine (BrdU, Sigma Aldrich) dissolved in DMSO/saline at a dose of 100 mg/kg bodyweight [64]. All animals had free access to drinking water and were maintained on the same standard diet. All animal experiments were performed according to national and international guidelines and Swiss laws of animal welfare and protocols approved by the local Veterinary Authority (Veterinäramt Zurich).

Immunoblotting

Mice were anesthetized with ketamine-xylazine and perfused through the left heart ventricle with warm (37°C) sucrose/ phosphate buffer (140 mM sucrose, 28 mM NaH_2PO_4, 112 mM Na_2HPO_4, pH 7.4). Kidneys were rapidly removed, frozen in liquid nitrogen, and placed at -80°C until further analysis. For total membrane preparation one kidney of each mouse was homogenized in an ice-cold K-HEPES buffer (200 mM mannitol, 80 mM HEPES, 41 mM KOH, pH 7.5) containing a protease inhibitor mix (complete Mini, Roche Diagnostics, Germany) at a final concentration of 1 tablet in a volume of 10 ml solution. Samples were centrifuged at 2000 rpm for 20 min at 4°C. Subsequently, the supernatant was transferred to a new tube and centrifuged at 41000 rpm for 1 h at 4°C. The resultant pellet was resuspended in K-HEPES buffer containing protease inhibitors. After measurement of the total protein concentration (Bio-Rad D_c Protein Assay; Bio-Rad, Hercules, CA, USA), 50 µg of the total membrane fraction was solubilized in Laemmli sample buffer, and SDS-PAGE was performed on 8-12 % polyacrylamide gels. For immunoblotting, proteins were transferred electrophoretically to polyvinylidene difluoride membranes (Immobilon-P, Millipore, Bedford, MA, USA). After blocking with 5% milk powder in Tris-buffered saline/ 0.1% Tween-20 for 60min, the blots were incubated with the respective primary antibodies

(rabbit anti-pendrin 1:5'000 [20], rabbit anti-AE1 1:10'000 [45], rabbit anti-AQP2 1:10'000 (kindly provided by Dr. J. Loffing, Institute of Anatomy, University of Zurich, [56]), and mouse monoclonal anti-β-actin antibody (42 kDa; Sigma, St. Louis, MO, USA) 1:10'000, all diluted in 1% milk/ TBS-Tween) either for 2 hrs at room temperature or overnight at 4°C. After washing and subsequent blocking, the membranes were incubated for 1 h at room temperature with the secondary antibody (donkey anti-rabbit or sheep anti-mouse antibodies linked to horseradish peroxidase 1:10'000 (GE Healthcare, Little Chalfont, Buckinghamshire, UK) or goat anti-rabbit antibody 1:5'000 linked to alkaline phosphatase (Promega, Madison, WI). Antibody binding was detected with the Immobilon Western Chemiluminescence kit (Millipore, Billerica, MA), using the DIANA III-chemiluminescence detection system (Raytest, Straubenhardt, Germany). All images were analyzed using appropriate software (Advanced Image Data Analyzer, Raytest) to calculate the protein of interest/ actin ratio.

RNA extraction and semi-quantitative real-time RT-PCR

One half kidney of each mouse was homogenized in RLT-Buffer (Qiagen, Basel, Switzerland) containing 2-mercaptoethanol (Sigma, Buchs, Switzerland) at a final concentration of 1%. Total RNA was extracted from 200 µl aliquots of each homogenized sample using the RNeasy Mini Kit (Qiagen, Basel, Switzerland) according to the manufacturers' instructions. Quantity and quality of total eluted RNA were assessed by spectrometry using the ND-1000 spectrophotometer (NanoDrop Technologies, DE, USA). Each RNA sample was diluted to 100 ng/ µl, and 3 µl was used as a template for reverse transcription using the TaqMan Reverse Transcription Kit (Applied Biosystems, Foster City, CA, USA) according to manufacturers' protocol. Remaining RNA samples were stored at -80°C. Semi-quantitative real-time RT-PCR (qPCR) was performed on the ABI PRISM 7700 Sequence Detection System (Applied Biosystems, Foster City, CA, USA). Primers for all genes of interest were designed using Primer Express software from Applied Biosystems and primers and probes for AE1, AQP2 und Pendrin were used as described previously [30]. Novel primer and probe sequences were: Hprt (NM_013556): forward: 5'-TTATCAGACTGAAGAGCTACTGTAATGATC -3', reverse: 5'-TTACCAGTGTCAATTATATCTTCAACAATC -3', probe: 5'-TGAGAGATCATCTCCACCAATAACTTTTATGTCCC -3'; Cp2l1 (NM_023755): forward: 5'-ATGCTGTTCTGGCACACGCAGC -3', reverse: 5'- TCTCAGGAGATAGCTGCGGCTC -3',

probe: 5'- TGGCAGCTACTTGCGTGATGTGCTGGC -3'; Gdf-15 (NM_011819): forward: 5'- AGAGGACTCGAACTCAGAACCAAG -3', reverse: 5'- TTGACGCGGAGTAGCAGCTGGC -3', probe: 5'- TGTCCGGATACTCAGTCCAGAGGTGAGA -3'. All primer and probes were tested and resulted in the expected products (data not shown). Probes were labeled with the reporter dye FAM at the 5' end and the quencher dye TAMRA at the 3'end (Microsynth, Balgach, Switzerland). Real-time PCR reactions were performed using the TaqMan Universal PCR Master Mix (Applied Biosystems, Foster City, CA, USA). Briefly, a 25 µl PCR reaction volume was prepared using 3.5 µl cDNA as template with sense and antisense primers (25 µM each), the labeled probed (5 µM), the Taqman Universal PCR Master Mix and RNase free water up to the final volume. Thermal cycles were set for denaturation at 95°C (10 min) followed by 40 cycles of denaturation at 95°C (15 s) and annealing/ elongation at 60°C (1 min) with auto ramp time. All reactions were run in triplicates. To analyze the data, we set the threshold to 0.06 as this value had been determined to be in the linear range of the amplification curves for all mRNAs in all experimental runs. The expression of gene of interest was calculated in relation to hypoxanthine guanine phosphoribosyl transferase (HPRT). Relative expression ratios were calculated as $R = 2^{[Ct(HPRT) - Ct(test\ gene)]}$, where Ct represents the cycle number at the threshold 0.06.

Immunohistochemistry

For immunohistochemistry, mice were anesthetized by an intraperitoneal injection of xylazine/ketamine and fixed by perfusion through the left heart ventricle. The fixative contained 3% paraformaldehyde (PFA) in phosphate-buffered saline (pH 7.4). The kidneys were removed and further fixed in PFA/PBS overnight at 4°C. After washing in PBS, cutting in two-four millimeter thick slices and cryoprotection in 3 M sucrose/PBS, kidneys were frozen in liquid propane cooled down to -196°C by liquid nitrogen. Frozen kidney slices were cut into 4 µm thick cryostat sections. Cryosections were microwaved for 5 min in 0.01 M citrate buffer at pH 6.0, followed by antigen retrieval with 1% SDS for 3 min, and subsequent three times washing in PBS for 5 min. After pretreatment in 1 % Bovine Serum Albumin (BSA)/PBS, cryosections were incubated overnight in a humidified chamber at 4°C with the primary antibodies (guinea-pig anti-AE1 1:1'000 [45], guinea pig anti-pendrin 1:1'000 [20], goat anti-AQP2 (Santa Cruz) 1:400, mouse monoclonal anti-BrdU (BD Pharmingen) 1:100, rabbit anti-Ki67 (Clone SP6, Spring Bioscience, Cat #M3064, 1:400 diluted in PBS. After

incubation with primary antibodies, sections were rinsed three times with PBS and PBS/NaCl (18 g NaCl/l PBS) and covered for 1 h at room temperature in the dark with the appropriate secondary antibodies (donkey anti-rabbit Alexa 594 1:1000, donkey anti-guinea pig Alexa 488 1:500, donkey anti-mouse Cy5 1:500, donkey anti-goat Alexa 647 1:1000 (Invitrogen, Basel, Switzerland) and DAPI 1:500 (Sigma) at the given dilutions for 1 h at room temperature. For nuclear staining, 49,6-diamidino-2-phenylindole (DAPI; Sigma, St. Louis, MO, USA), diluted 1:500, was added to the secondary antibodies. Sections were again washed twice with high-NaCl-PBS and once with PBS before being mounted with Glycergel (DakoCytomation, Glostrup, Denmark). All sections from different animal groups within one series were processed simultaneously with the same dilutions of primary and secondary antibodies. Sections were viewed using a Leica DFC490 charged-coupled device camera attached to a Leica DM 6000 fluorescence microscope (Leica, Wetzlar, Germany) using equivalent camera parameters for all kidneys sections. Pictures were viewed and processed using Photoshop. Five animals per group (time and treatment) were processed and 20 cortical fields at 400x magnification were photographed. Only cells with clear labeling of either the luminal or basolateral side with the respective markers were included.

Statistical Analysis

All data are presented as means ± SEM and were tested for significance using one way ANOVA test. Results with $p < 0.05$ were considered statistically significant.

RESULTS

$NaHCO_3$ and NaCl-loading alter expression of intercalated cell specific transport proteins AE1 and Pendrin

Mice were treated for 12 or 24hrs and 2 or 7 days with $NaHCO_3$ to provide an alkali-load. In order to control for the effects of sodium loading, another group received equimolar amounts of NaCl for the same time periods. A third group was left untreated and received only standard chow. The $NaHCO_3$ diet has previously been shown to induce hypochloremic alkalemia with alkaline urine whereas NaCl imposes a mild acid load (as compared to untreated mice) and increases urinary sodium and chloride excretion [30].

We first tested the effect of treatments on the mRNA and protein expression of pendrin (Figure 1). Pendrin mRNA was higher in the $NaHCO_3$ group after 24 hrs compared to control and the NaCl group (Figure 1A). After 7 days, the NaCl group had lower pendrin mRNA abundance but this difference did not reach significance in ANOVA testing (Figure 1A). In all other groups and at all other time points no significant differences in pendrin mRNA abundance were detected. Pendrin protein abundance was also higher after 24 hrs and 7 days $NaHCO_3$ (Figures 1C and 1E).

mRNA expression of the type A intercalated cell specific anion exchanger AE1 did not change significantly after 12 hrs $NaHCO_3$ or after 2 days (Figure 2A). At the protein level, AE1 was elevated after 7 days NaCl (Figure 2E) but otherwise remained unchanged.

In contrast to AE1 and Pendrin, the expression of AQP2 was highly regulated. mRNA abundance showed significant differences/increase only after 24 hrs NaCl or $NaHCO_3$ loading without significant changes for all other time points (Figure 3A). AQP2 protein abundance was increased in the $NaHCO_3$ group after 24 hrs and 7 days (Figure 3C and E). Also, the NaCl treated group had higher AQP2 protein expression after 7 days (Figures 3C and E). Surprisingly, AQP2 protein was reduced after 2 days (Figure 3D).

Altered cellular profile in response to alkali loading

Kidney sections from control mice or mice treated for 12 hrs, 24 hrs or 7 days with $NaHCO_3$ or NaCl were stained with antibodies against the anion exchanger 1, AE1, as a marker of type A intercalated cells [4], against pendrin, as a marker of type B and non-A/non-B intercalated cells [40,59], and against AQP2, as a marker of principal cells [31]. The

relative abundance of the different cell types were counted in the cortical collecting system comprising of the connecting tubule and cortical collecting duct in order to assess the impact of the different treatments on cellular remodeling. As summarized in table 1, both diets had no impact on the relative abundance of AQP2-positive cells in the cortical collecting system. After 7 days, $NaHCO_3$ increased the relative abundance of pendrin-positive cells in the cortical collecting system compared to control or NaCl-treated mice. Concomitantly, the relative abundance of AE1-positive type A intercalated cells was significantly reduced. Thus, $NaHCO_3$-loading alters the cellular profile in the cortical collecting system by increasing the relative number of pendrin-expressing cells at the expense of AE1-positive type A intercalated cells.

Alkali and NaCl loading induce changes in transcription factors and cell proliferation

Next, we tested the effects of the different treatments on the mRNA abundance of several factors that have been shown to modulate the differentiation and/or relative abundance of the different cell types along the collecting duct system. CP2L1 mRNA expression showed a non-significant reduction after 12 hrs Interestingly, after 24 hrs the NaCl group had higher CP2L1 levels (Figure 4A). In contrast, the forkhead transcription factor Foxi1 showed a transient increase in the $NaHCO_3$-treated group peaking after 24 hrs (Figure 4B). Also, GDF-15 mRNA abundance increased after 24 hrs and 2 days in the $NaHCO_3$-treated group and returned to baseline after 7 days (Figure 4C).

We then analyzed the association of proliferation of specific cells during the treatment with NaCl or $NaHCO_3$. Animals used for examining the cellular remodeling of the CNT and CCD had been injected with BrdU, which is incorporated into DNA during synthesis and labels cells that undergo cell division. BrdU staining was combined with the specific cell markers AE1, pendrin and AQP2 and BrdU-positive cell nuclei were counted as summarized in table 1 and shown in figure 5. BrdU-positive cells were found in all groups of animals and were mostly associated with AQP2 staining (besides BrdU staining in regions of the kidney other than the cortical collecting system, data not shown) but also sporadically found in AE1- or pendrin-positive cells consistent with earlier reports (Figure 5E) [62]. Treatment of mice with NaCl or $NaHCO_3$ increased the relative number of BrdU- and AQP2-positive cells in the cortical collecting system after 7 days (table 1). In order to further corroborate the association of cell proliferation with AQP2 expression, kidney sections were stained for pendrin, AQP2 and Ki67, a marker of proliferating cells. The lack of a positive marker for type A intercalated

cells tended to underestimate the relative abundance of these cells (identified by the absence of pendrin and AQP2 staining). However, with the antibodies available to us, we could not simultaneously stain for all markers and decided to mainly focus on the detection of proliferation of AQP2 positive cells. We examined only two time points, 24 hrs and 7 days after induction of diets (Figure 6, table 2). In control animals only few cortical collecting duct cells that did not stain for AQP2 or pendrin showed Ki67 staining suggesting a very low rate of proliferation of type A intercalated cells. Pendrin positive cells showed only in a very few cases Ki67 staining. In contrast, 3-4 % of AQP2 positive cells were Ki67 positive (Figure 6, table 2). Induction of $NaHCO_3$ loading significantly increased the relative abundance of Ki67 and AQP2 positive cells after 24 hrs (table 2).

DISCUSSION

The collecting duct is the main site of regulated acid or base excretion adapting to the metabolic and systemic acid-base status of the individuum [54,21]. All three major cell types along the collecting duct system are involved in this context. Each cell type is characterized by a distinct set of proteins expressed reflecting specific cellular functions [10]. Type A intercalated cells secrete protons through apically located H^+-ATPases and release bicarbonate into blood via the basolateral chloride/bicarbonate exchanger AE1. Proton secretion is paralleled by ammonia secretion through the RhCG ammonia channel expressed in principal cells, type A and type B intercalated cells (albeit with some differences in subcellular localization) [52]. Bicarbonate secretion depends on type B intercalated cells expressing the chloride/bicarbonate exchanger pendrin and basolaterally and /or apically located H^+-ATPases. Collecting duct acid or base excretion is adapted by the regulation of the activity as well as by changes in the relative abundance of the different subtypes of cells. While our understanding of mechanisms driving the adaption to acid-loading has made major advances over the past years, the mechanisms responsible for adaption to alkali have remained less well defined.

Here we find that 1) acute $NaHCO_3$ loading for 24 hrs transiently stimulated pendrin mRNA and protein expression, 2) both NaCl and $NaHCO_3$-loading altered AQP2 protein abundance, 3) chronic $NaHCO_3$ loading for 7 days increased the relative abundance of pendrin-positive type B intercalated cells at the expense of AE1-positive type A intercalated cells in the cortical collecting system, 4) $NaHCO_3$ loading acutely reduced mRNA levels of CP2L1, and transiently increased Foxi1 and GDF-15 levels, and 5) $NaHCO_3$ and NaCl-loading may have stimulated proliferation in the cortical collecting system as suggested from an increase in the relative number of Ki67 or BrdU-positive AQP2-expressing cells.

Our data suggest that several mechanisms may contribute to collecting duct adaption to alkali loading that may include increased pendrin protein expression per cell as indicated by higher pendrin protein levels without change in the relative number of pendrin expressing cells, and the increase in pendrin expressing cells as suggested by the higher frequency of pendrin-positive cells after 7 days. However, total pendrin protein abundance and the relative number of pendrin expressing cells does not take into account changes in pendrin transport activity that likely involves trafficking into and out of the luminal membrane and changes in transport activity per se. In fact, alkali loading stimulates pendrin staining at the luminal membrane [36,55]. Pendrin activity is regulated by β-adrenergic stimulation or by pH

[6,7]. Also a regulation of pendrin by the hydroxyl-activated Insulin receptor related receptor (Ins-RRR) has been suggested [35]. Whether these mechanism are active during alkalosis has not been fully resolved. In our study, increased pendrin protein expression was paralleled by higher pendrin mRNA abundance suggesting that transcriptional regulation may be involved. However, little is known about the transcriptional regulation of pendrin. Promoter activity of pendrin is enhanced by alkaline pH and decreased by acidic pH, a mechanism that could contribute to the changes observed here [1,41]. In addition, the forkhead transcription factor Foxi1 is critical for pendrin transcription both in kidney and inner ear [8,9,22,53]. In our experiments, increased abundance of Foxi1 mRNA coincides with higher pendrin mRNA after 24 hrs of $NaHCO_3$-loading providing a possible molecular explanation for enhanced pendrin expression at this time point.

Both NaCl and $NaHCO_3$ loading increased expression of the AQP2 water channel, mostly on protein level. This effect occurred as early as 24 hrs after starting the treatment and was pronounced after 24 hrs and 7 days in $NaHCO_3$-treated animals. At the intermediate time point, lower AQP2 levels in the NaCl group and unchanged levels in the $NaHCO_3$ group were observed. The reason for this transient change remains elusive at this point. Regulation of AQP2 has been observed in other animal models of acid-base disturbances such as mouse and rat models loaded with NH_4Cl in drinking water [32]. Strikingly, the upregulation and phosphorylation of AQP2 depended on the route of NH_4Cl administration, e.g. via drinking water or via food, and was not the consequence of acidosis *per se*. Since also NaCl treatment induced similar changes in AQP2 expression as $NaHCO_3$-loading, we speculate that sodium loading per se, reduced water consumption, intake of osmotically active substrates, or increased urinary flow may account for the effect observed here.

$NaHCO_3$-loading for 7 days was associated with a higher relative abundance of pendrin positive cells in the cortical collecting system, which was at least in part at the expense of AE1-expressing cells (table 1). Similar remodeling of the collecting duct has been reported in acid-loaded animals including mice, rats and rabbits where acid-loading induced an increase in the relative abundance of type A intercalated cells expressing AE1 [12,63,2,16]. In mice and rats, this type of collecting duct remodeling was paralleled by increased BrdU incorporation of Ki67 staining in AE1-positive cells suggesting that proliferation of type A intercalated cells may occur and contribute to remodeling. Moreover, GDF15 was required for the early phase of proliferation in mice challenged with acid-loading [12]. In our study, we did not find evidence for a significant BrdU incorporation in pendrin

expressing cells or an effect of alkali or NaCl loading on this parameter. Only very few pendrin-expressing cells showed BrdU incorporation which was comparable to BrdU incorporation in AE1 expressing cells but much less frequent than in AQP2 positive cells. However, a previous study reported BrdU incorporation in all cell types along the murine collecting duct system of animals without any challenge and increased incorporation in non-type A intercalated cells in animals treated with loop-diuretics [62]. We thus tested also for the presence of Ki67, a marker of proliferating cells. Also Ki67 staining was most prominent in AQP2 expressing cells and only very few cells either negative for AQP2 and pendrin (i.e. type A intercalated cells) or positive for pendrin (i.e. type B intercalated cells) showed Ki67 staining. In contrast, $NaHCO_3$-loading significantly increased the relative number of Ki67 positive AQP2-expressing cells after 24 hrs suggesting that $NaHCO_3$-loading provides a proliferative stimulus. The discrepancy between our study and the previous study reporting BrdU labeling of pendrin positive cell may be in part explained by a relatively low number of BrdU incorporating cells in our study suggesting that not all cells incorporated enough BrdU to be detected. This interpretation is also supported by a higher number of Ki67 positive cells in our study which should be in fact lower than the number of BrdU positive cells after 7 days. Of note, the sample size of the different groups (i.e. cells counted) used to detect ki67 or BrdU positive cells considerably differed which may have introduced a bias to overestimate the presence of ki67 or BrdU positive AQP2-expressing cells. Nevertheless, our findings suggest that proliferation of pendrin-positive cells does not contribute to collecting duct remodeling, or other cells such AQP2-expressing cells proliferate and are then transformed to pendrin-positive cells. The latter model would be consistent with the apparent higher rate of BrdU and Ki67 staining in APQ2-expressing cells and recent cell-fate mapping results suggesting that AQP2 positive cells can give rise to type B intercalated cells [49]. Clearly, the origin of the relative increase in pendrin positive cells remains to be further clarified.

Recent single cell transcriptome data from mouse kidney described a novel cell type that may be transiting between principal and intercalated cells. This cell type expresses mRNA for AQP2, pendrin, AE1, Foxi1, and Tfcp2l1 [33,38,10]. However, the relative abundance of this cell type is unclear and ranged in two reports between less than 0.5 and 4 % of all collecting duct cells and might even represent cell doublets from incomplete dissocation during single cell collection [33,38]. Cell-marker mapping in rats undergoing 14 days of potassium depletion or rats treated for 19 days with lithium demonstrated the occurrence of cells positive for markers of both principal and intercalated cells suggesting

the existence of a hybrid cell type or transition from one cell type to another [23,48]. Here, we had specifically searched for cells coexpressing AQP2 and pendrin or AE1 but failed to unequivocally detect any.

Maturation, cell patterning, and remodeling of the complex composition of the collecting duct is driven and determined by a network of factors that has started to emerge only recently. Major factors include Foxi1, CP2L1 (also known as TFCP2L1), Notch2/Jag1, Adam10, and the grainyhead-like 2/Ovo-like 2 even though the exact relationship and target genes have not been fully elucidated [25,18,29,8,37,68,5,65]. Moreover, additional factors like hensin (DMBT1), GDF15, or SDF1 modulate the relative abundance of specific cell subtypes in response to metabolic changes such as acid-loading [43,12,16]. We tested the regulation of CP2L1, Foxi1, and GDF-15 during alkali-loading and found a transient suppression of CP2L1 and transient increase in Foxi1 and GDF-15 although regulation of all three factors was not specific for $NaHCO_3$-loading at all time points (e.g. CP2L1 regulation by NaCl-loading after 24 hrs and possibly 7 days). The Xenopus laevis homologue of CP2L1, ubp1, suppresses differentiation of type A intercalated cell like cells in frog skin [37]. The downregulation of CP2L1 observed here might thus contribute to the stimulation of type B intercalated cell activity or expansion. In contrast, Foxi1 may act upstream of CP2L1 and induce differentiation of cells towards the intercalated cell lineage [8] with a potential preference towards type A intercalated cells [37]. Consequently, loss of Foxi1 causes a cell type that expresses markers of both the principal and intercalated cell lineage in mice and causes distal renal tubular acidosis in humans [8,14]. Notably, pendrin is also among the transcriptional targets of Foxi1 [22,53]. Thus, the combined increase in Foxi1 and decrease in CP2L1 could lead to increased differentiation towards type B intercalated cells. However, the exact role of these two transcription factors in the adaptation of the collecting duct to alkali-loading will require more detailed analyses using cell-specific localization of their activity and genetic deletion. Single cell transcriptome analysis of the developing kidney suggests a special role of Hox genes in patterning particularly the junction between CNT and CCD and that Hox10 expressing cells may give rise to both intercalated and principal cell like cells [38]. Whether Hox genes play a role in the adaptive remodeling of the collecting duct during acid or alkali loading remains to be tested.

Our study is limited by the lack of direct evidence for the role of cell proliferation in the adaptation of the collecting duct system which may require cell-fate mapping or other more detailed methods such as whole organ based immunohistochemistry to further trace

origin and plasticity of cells along the collecting duct system. The use of mice labeling AQP2 positive cells with YFP has been reported and would provide a model to further analyze the role of principal cells as possible precursor of (type B) intercalated cells in the adaption to alkalosis [49]. Our approach did also not take into consideration changes in the overall architecture of the collecting duct system such as total cell number or cell size. This could be further addressed by detailed histomorphometry or whole organ based techniques such as combining cell specific markers with clearing the organ for whole mount imaging (i.e CLARITY approaches) [42]. Last, our data provide only associations for the regulation of various (transcription) factors with remodeling but at this point no definite proof for their role can be demonstrated which would require timed and cell-specific blocking or deletion of these factors. These experiments were beyond the scope and possibilities of our study and need to be addressed in future studies.

In summary, alkali-loading in mice stimulates type B intercalated cells causing a transient increase in pendrin expression and a shift towards a higher relative abundance of type B intercalated cells. These changes are preceded and paralleled by changes in Foxi1, CP2L1, and GDF-15, factors involved in collecting duct patterning and cell proliferation. However, the exact role of these factors as well as of other mechanisms underlying the adaptation to alkalosis remain to be further defined.

FIGURES LEGENDS

Table 1

Summary of relative frequencies or numbers (in percent) of cells positive for AE1 or AE1 plus BrdU, for pendrin or pendrin plus BrdU, and for AQP2 or AQP2 plus BrdU in kidneys from control mice or mice receiving either 0.28 M $NaHCO_3$ or 0.28 M NaCl for 12 hrs, 24 hrs, or 7 days. Five mice per group and time point were treated and sections analyzed, n denotes the number of cells counted in all kidneys from this group. *$p < 0.05$ denotes differences between groups for the same time point.

Table 2

Summary of relative frequencies or numbers (in percent) of cells positive for AE1 or AE1 plus Ki67 for pendrin or pendrin plus Ki67, and for AQP2 or AQP2 plus Ki67in kidneys from control mice or mice receiving either 0.28 M $NaHCO_3$ or 0.28 M NaCl for 24 hrs and 7 days. Five mice per group and time point were treated and sections analyzed, n denotes the number of cells counted in all kidneys from this group. *$p < 0.05$ denotes differences between groups for the same time point.

Figure 1: **Regulated Pendrin expression.** Pendrin mRNA and protein abundance was tested in total kidneys from control mice and mice receiving 0.28 M $NaHCO_3$ or 0.28 M NaCl for 12 hrs, 24 hrs, 2 or 7 days. **(A)** Relative mRNA abundance of Pendrin (normalized to the respective control groups). (**B-E**) Western blotting of total membrane fractions for pendrin. Membranes were stripped and reprobed for β-actin. Bar graphs show relative pendrin abundance normalized to β-actin. Mean ± S.E.M, n = 5 for each group and condition, *$p < 0.05$, **$p < 0.01$, ***$p < 0.001$.

Figure 2: Regulated AE1 expression. AE1 mRNA and protein abundance was tested in total kidneys from control mice and mice receiving 0.28 M $NaHCO_3$ or 0.28 M NaCl for 12 hrs, 24 hrs, 2 or 7 days. **(A)** Relative mRNA abundance of AE1 (normalized to the respective control groups). (**B-E**) Western blotting of total membrane fractions for AE1. Membranes were stripped and reprobed for β-actin. Bar graphs show relative AE1 abundance

normalized to β-actin. Mean ± S.E.M, n = 5 for each group and condition, *p < 0.05, **p < 0.01.

Figure 3: Regulated AQP2 expression. AQP2 mRNA and protein abundance was tested in total kidneys from control mice and mice receiving 0.28 M $NaHCO_3$ or 0.28 M NaCl for 12 hrs, 24 hrs, 2 or 7 days. **(A)** Relative mRNA abundance of AQP2 (normalized to the respective control groups). (**B-E**) Western blotting of total membrane fractions for AQP2. Membranes were stripped and reprobed for β-actin. Bar graphs show relative AQP2 abundance normalized to β-actin. Mean ± S.E.M, n = 5 for each group and condition, **p < 0.01, ***p < 0.001.

Figure 4: mRNA expression of key factors implied in intercalated cells differentiation. mRNA abundance of Foxi1, GDF-15, and CP2L1 was tested in total kidneys from control mice and mice receiving 0.28 M $NaHCO_3$ or 0.28 M NaCl for 12 hrs, 24 hrs, 2 or 7 days. mRNA abundance was normalized to the respective control groups. Mean ± S.E.M, n = 5 for each group and condition, *p < 0.05, **p < 0.01, ***p < 0.001.

Figure 5: Proliferation of cells in the cortical collecting system. Kidney sections from control mice and mice receiving 0.28 M $NaHCO_3$ or 0.28 M NaCl for 7 days and injected daily with BrdU were stained with antibodies against BrdU (green), AE1 (green), Pendrin (red), AQP2 (white), and with DAPI (blue). Arrows indicate BrdU positive cell nuclei, inserts show higher magnification of cells with BrdU labeling. **(A,B)** Kidneys from untreated control mice, **(C,D)** kidneys from mice receiving $NaHCO_3$ for 7 days, and **(E,F)** kidneys from mice receiving NaCl for 7 days. Original magnification 400-630x.

Figure 6: Proliferation of cells in the cortical collecting system. Kidney sections from control mice and mice receiving 0.28 M $NaHCO_3$ or 0.28 M NaCl for 24 hrs or 7 days were stained with antibodies against Ki67 (red), Pendrin (green), AQP2 (white), and with DAPI (blue). Arrows indicate Ki67 positive cell nuclei, inserts show higher magnification of cells

with Ki67 labeling. **(A-C)** Kidneys from mice after 24 hrs of treatment and control, **(D-F)** kidneys from mice receiving treated for 7 days. Original magnification 400x.

REFERENCES

1. Adler L, Efrati E, Zelikovic I (2008) Molecular mechanisms of epithelial cell-specific expression and regulation of the human anion exchanger (pendrin) gene. Am J Physiol Cell Physiol 294:C1261-1276

2. Al-Awqati Q (2003) Terminal differentation of intercalated cells: The role of Hensin. Annu Rev Physiol 65:567-583

3. Al-Awqati Q (2011) Terminal differentiation in epithelia: the role of integrins in hensin polymerization. Annu Rev Physiol 73:401-412. doi:10.1146/annurev-physiol-012110-142253

4. Alper SL, Natale J, Gluck S, Lodish HF, Brown D (1989) Subtypes of intercalated cells in rat kidney collecting duct defined by antibodies against erythroid band 3 and renal vacuolar H^+-ATPase. Proc Natl Acad Sci U S A 86:5429-5433

5. Aue A, Hinze C, Walentin K, Ruffert J, Yurtdas Y, Werth M, Chen W, Rabien A, Kilic E, Schulzke JD, Schumann M, Schmidt-Ott KM (2015) A Grainyhead-Like 2/Ovo-Like 2 Pathway Regulates Renal Epithelial Barrier Function and Lumen Expansion. J Am Soc Nephrol 26:2704-2715. doi:ASN.2014080759 [pii]

10.1681/ASN.2014080759

6. Azroyan A, Laghmani K, Crambert G, Mordasini D, Doucet A, Edwards A (2011) Regulation of pendrin by pH: dependence on glycosylation. Biochem J 434:61-72. doi:BJ20101411 [pii]

10.1042/BJ20101411

7. Azroyan A, Morla L, Crambert G, Laghmani K, Ramakrishnan S, Edwards A, Doucet A (2012) Regulation of pendrin by cAMP: possible involvement in beta-adrenergic-dependent NaCl retention. Am J Physiol Renal Physiol 302:F1180-1187. doi:ajprenal.00403.2011 [pii]

10.1152/ajprenal.00403.2011

8. Blomqvist SR, Vidarsson H, Fitzgerald S, Johansson BR, Ollerstam A, Brown R, Persson AE, Bergstrom GG, Enerback S (2004) Distal renal tubular acidosis in mice that lack the forkhead transcription factor Foxi1. J Clin Invest 113:1560-1570

9. Blomqvist SR, Vidarsson H, Soder O, Enerback S (2006) Epididymal expression of the forkhead transcription factor Foxi1 is required for male fertility. Embo J 25:4131-4141

10. Chen L, Lee JW, Chou CL, Nair AV, Battistone MA, Paunescu TG, Merkulova M, Breton S, Verlander JW, Wall SM, Brown D, Burg MB, Knepper MA (2017) Transcriptomes of major renal collecting duct cell types in mouse identified by single-cell RNA-seq. Proc Natl Acad Sci U S A. doi:1710964114 [pii]

10.1073/pnas.1710964114

11. Christensen EI, Wagner CA, Kaissling B (2012) Uriniferous tubule: structural and functional organization. Compr Physiol 2:805-861. doi:10.1002/cphy.c100073

12. Duong Van Huyen JP, Cheval L, Bloch-Faure M, Belair MF, Heudes D, Bruneval P, Doucet A (2008) GDF15 triggers homeostatic proliferation of acid-secreting collecting duct cells. J Am Soc Nephrol 19:1965-1974. doi:ASN.2007070781 [pii]

10.1681/ASN.2007070781

13. El-Dahr SS, Aboudehen K, Saifudeen Z (2008) Transcriptional control of terminal nephron differentiation. Am J Physiol Renal Physiol 294:F1273-1278. doi:00562.2007 [pii]

10.1152/ajprenal.00562.2007

14. Enerback S, Nilsson D, Edwards N, Heglind M, Alkanderi S, Ashton E, Deeb A, Kokash FEB, Bakhsh ARA, Van't Hoff W, Walsh SB, D'Arco F, Daryadel A, Bourgeois S, Wagner CA, Kleta R, Bockenhauer D, Sayer JA (2017) Acidosis and Deafness in Patients with Recessive Mutations in FOXI1. J Am Soc Nephrol. doi:ASN.2017080840 [pii]

10.1681/ASN.2017080840

15. Galla JH, Gifford JD, Luke RG, Rome L (1991) Adaptations to chloride-depletion alkalosis. Am J Physiol 261:R771-781

16. Gao X, Eladari D, Leviel F, Tew BY, Miro-Julia C, Cheema F, Miller L, Nelson R, Paunescu TG, McKee M, Brown D, Al-Awqati Q (2010) Deletion of hensin/DMBT1 blocks conversion of {beta}- to {alpha}-intercalated cells and induces distal renal tubular acidosis. Proc Natl Acad Sci U S A. doi:1010364107 [pii]

10.1073/pnas.1010364107

17. Gueutin V, Vallet M, Jayat M, Peti-Peterdi J, Corniere N, Leviel F, Sohet F, Wagner CA, Eladari D, Chambrey R (2013) Renal beta-intercalated cells maintain body fluid and electrolyte balance. J Clin Invest 123:4219-4231. doi:63492 [pii]

10.1172/JCI63492

18. Guo Q, Wang Y, Tripathi P, Manda KR, Mukherjee M, Chaklader M, Austin PF, Surendran K, Chen F (2015) Adam10 mediates the choice between principal cells and intercalated cells in the kidney. J Am Soc Nephrol 26:149-159. doi:ASN.2013070764 [pii]

10.1681/ASN.2013070764

19. Hadchouel J, Busst C, Procino G, Valenti G, Chambrey R, Eladari D (2011) Regulation of extracellular fluid volume and blood pressure by pendrin. Cell Physiol Biochem 28:505-512. doi:000335116 [pii]

10.1159/000335116

20. Hafner P, Grimaldi R, Capuano P, Capasso G, Wagner CA (2008) Pendrin in the mouse kidney is primarily regulated by Cl- excretion but also by systemic metabolic acidosis. Am J Physiol Cell Physiol 295:C1658-1667

21. Hamm LL, Alpern RJ, Preisig PA (2008) Cellular mechanisms of renal tubular acidification. In: Alpern RJ, Hebert SC (eds) Seldin and Giebisch's The Kidney. Physiology and Pathophysiology. 4th edn. Academic Press, pp 1539-1585

22. Hulander M, Kiernan AE, Blomqvist SR, Carlsson P, Samuelsson EJ, Johansson BR, Steel KP, Enerback S (2003) Lack of pendrin expression leads to deafness and expansion of the endolymphatic compartment in inner ears of Foxi1 null mutant mice. Development 130:2013-2025

23. Iervolino A, Prosperi F, De La Motte LR, Petrillo F, Spagnuolo M, D'Acierno M, Siccardi S, Perna AF, Christensen BM, Frische S, Capasso G, Trepiccione F (2020) Potassium depletion induces cellular conversion in the outer medullary collecting duct altering Notch signaling pathway. Sci Rep 10:5708. doi:10.1038/s41598-020-61882-7

24. Jacques T, Picard N, Miller RL, Riemondy KA, Houillier P, Sohet F, Ramakrishnan SK, Busst CJ, Jayat M, Corniere N, Hassan H, Aronson PS, Hennings JC, Hubner CA, Nelson RD, Chambrey R, Eladari D (2013) Overexpression of pendrin in intercalated cells produces chloride-sensitive hypertension. J Am Soc Nephrol 24:1104-1113. doi:ASN.2012080787 [pii]

10.1681/ASN.2012080787

25. Jeong HW, Jeon US, Koo BK, Kim WY, Im SK, Shin J, Cho Y, Kim J, Kong YY (2009) Inactivation of Notch signaling in the renal collecting duct causes nephrogenic diabetes insipidus in mice. J Clin Invest 119:3290-3300. doi:38416 [pii]

10.1172/JCI38416

26. Kim J, Kim, Y H, Cha, J H, Tisher, C C, Madsen, K M (1999) Intercalated cell subtypes in connecting tubule and cortical collecting duct of rat and mouse. J Am Soc Nephrol 10:1-12

27. Leviel F, Hubner CA, Houillier P, Morla L, El Moghrabi S, Brideau G, Hassan H, Parker MD, Kurth I, Kougioumtzes A, Sinning A, Pech V, Riemondy KA, Miller RL, Hummler E, Shull GE, Aronson PS, Doucet A, Wall SM, Chambrey R, Eladari D (2010) The Na+-dependent chloride-bicarbonate exchanger SLC4A8 mediates an electroneutral Na+ reabsorption process in the renal cortical collecting ducts of mice. J Clin Invest 120:1627-1635. doi:40145 [pii]

10.1172/JCI40145

28. Loffing J, Kaissling, B (2003) Sodium and calcium transport pathways along the mammalian distal nephron: from rabbit to human. Am J Physiol Renal Physiol 284:F628-643

29. McCright B, Lozier J, Gridley T (2002) A mouse model of Alagille syndrome: Notch2 as a genetic modifier of Jag1 haploinsufficiency. Development 129:1075-1082

30. Mohebbi N, Perna A, van der Wijst J, Becker HM, Capasso G, Wagner CA (2013) Regulation of two renal chloride transporters, AE1 and pendrin, by electrolytes and aldosterone. PLoS One 8:e55286. doi:10.1371/journal.pone.0055286

PONE-D-12-33567 [pii]

31. Nielsen S, DiGiovanni, S R, Christensen, E I, Knepper, M A, Harris, H W (1993) Cellular and subcellular immunolocalization of vasopressin-regulated water channel in rat kidney. Proc Natl Acad Sci USA 90:11663-11667

32. Nowik M, Kampik NB, Mihailova M, Eladari D, Wagner CA (2010) Induction of metabolic acidosis with ammonium chloride (NH4Cl) in mice and rats--species differences and technical considerations. Cell Physiol Biochem 26:1059-1072. doi:000323984 [pii]

10.1159/000323984

33. Park J, Shrestha R, Qiu C, Kondo A, Huang S, Werth M, Li M, Barasch J, Susztak K (2018) Single-cell transcriptomics of the mouse kidney reveals potential cellular targets of kidney disease. Science 360:758-763. doi:10.1126/science.aar2131

34. Patel N, Sharpe PT, Miletich I (2011) Coordination of epithelial branching and salivary gland lumen formation by Wnt and FGF signals. Dev Biol 358:156-167. doi:S0012-1606(11)01141-9 [pii]

10.1016/j.ydbio.2011.07.023

35. Petrenko AG, Zozulya SA, Deyev IE, Eladari D (2013) Insulin receptor-related receptor as an extracellular pH sensor involved in the regulation of acid-base balance. Biochim Biophys Acta 1834:2170-2175. doi:S1570-9639(12)00268-3 [pii]

10.1016/j.bbapap.2012.11.011

36. Purkerson JM, Tsuruoka S, Suter DZ, Nakamori A, Schwartz GJ (2010) Adaptation to metabolic acidosis and its recovery are associated with changes in anion exchanger distribution and expression in the cortical collecting duct. Kidney Int 78:993-1005. doi:ki2010195 [pii]

10.1038/ki.2010.195

37. Quigley IK, Stubbs JL, Kintner C (2011) Specification of ion transport cells in the Xenopus larval skin. Development 138:705-714. doi:138/4/705 [pii]

10.1242/dev.055699

38. Ransick A, Lindstrom NO, Liu J, Zhu Q, Guo JJ, Alvarado GF, Kim AD, Black HG, Kim J, McMahon AP (2019) Single-Cell Profiling Reveals Sex, Lineage, and Regional Diversity in the Mouse Kidney. Dev Cell 51:399-413 e397. doi:10.1016/j.devcel.2019.10.005

39. Roy A, Al-bataineh MM, Pastor-Soler NM (2015) Collecting duct intercalated cell function and regulation. Clin J Am Soc Nephrol 10:305-324. doi:10.2215/CJN.08880914

40. Royaux IE, Wall, S M, Karniski, L P, Everett, L A, Suzuki, K, Knepper, M A, Green, E D (2001) Pendrin, encoded by the Pendred syndrome gene, resides in the apical region of renal intercalated cells and mediates bicarbonate secretion. Proc Natl Acad Sci U S A 98:4221-4226

41. Rozenfeld J, Efrati E, Adler L, Tal O, Carrithers SL, Alper SL, Zelikovic I (2011) Transcriptional regulation of the pendrin gene. Cell Physiol Biochem 28:385-396. doi:000335100 [pii]

10.1159/000335100

42. Saritas T, Puelles VG, Su XT, McCormick JA, Welling PA, Ellison DH (2018) Optical Clearing in the Kidney Reveals Potassium-Mediated Tubule Remodeling. Cell Rep 25:2668-2675 e2663. doi:10.1016/j.celrep.2018.11.021

43. Schwartz GJ, Gao X, Tsuruoka S, Purkerson JM, Peng H, D'Agati V, Picard N, Eladari D, Al-Awqati Q (2015) SDF1 induction by acidosis from principal cells regulates intercalated cell subtype distribution. J Clin Invest 125:4365-4374. doi:80225 [pii]

10.1172/JCI80225

44. Sinning A, Radionov N, Trepiccione F, Lopez-Cayuqueo KI, Jayat M, Baron S, Corniere N, Alexander RT, Hadchouel J, Eladari D, Hubner CA, Chambrey R (2016) Double Knockout of the Na+-Driven Cl-/HCO3- Exchanger and Na+/Cl- Cotransporter Induces Hypokalemia and Volume Depletion. J Am Soc Nephrol. doi:ASN.2015070734 [pii]

10.1681/ASN.2015070734

45. Stehberger PA, Shmukler BE, Stuart-Tilley AK, Peters LL, Alper SL, Wagner CA (2007) Distal renal tubular acidosis in mice lacking the AE1 (band3) Cl^-/HCO_3^- exchanger (slc4a1). J Am Soc Nephrol 18:1408-1418.

46. Surendran K, Boyle S, Barak H, Kim M, Stomberski C, McCright B, Kopan R (2010) The contribution of Notch1 to nephron segmentation in the developing kidney is revealed in a sensitized Notch2 background and can be augmented by reducing Mint dosage. Dev Biol 337:386-395. doi:10.1016/j.ydbio.2009.11.017

47. Teng-umnuay P, Verlander, J W, Yuan, W, Tisher, C C, Madsen, K M (1996) Identification of distinct subpopulations of intercalated cells in the mouse collecting duct. J Am Soc Nephrol 7:260-274

48. Trepiccione F, Capasso G, Nielsen S, Christensen BM (2013) Evaluation of cellular plasticity in the collecting duct during recovery from lithium-induced nephrogenic diabetes insipidus. Am J Physiol Renal Physiol 305:F919-929. doi:10.1152/ajprenal.00152.2012

49. Trepiccione F, Soukaseum C, Iervolino A, Petrillo F, Zacchia M, Schutz G, Eladari D, Capasso G, Hadchouel J (2016) A fate-mapping approach reveals the composite origin of the connecting tubule and alerts on "single-cell"-specific KO model of the distal nephron. Am J Physiol Renal Physiol 311:F901-F906. doi:10.1152/ajprenal.00286.2016

50. Verlander JW, Kim YH, Shin W, Pham TD, Hassell KA, Beierwaltes WH, Green ED, Everett L, Matthews SW, Wall SM (2006) Dietary Cl(-) restriction upregulates pendrin expression within the apical plasma membrane of type B intercalated cells. Am J Physiol Renal Physiol 291:F833-839

51. Verlander JW, Madsen, K M, Galla, J H, Luke, R G, Tisher, C C (1992) Response of intercalated cells to chloride depletion metabolic alkalosis. Am J Physiol 262:F309-319

52. Verlander JW, Miller RT, Frank AE, Royaux IE, Kim YH, Weiner ID (2003) Localization of the ammonium transporter proteins RhBG and RhCG in mouse kidney. Am J Physiol Renal Physiol 284:F323-337

53. Vidarsson H, Westergren R, Heglind M, Blomqvist SR, Breton S, Enerback S (2009) The forkhead transcription factor Foxi1 is a master regulator of vacuolar H-ATPase proton pump subunits in the inner ear, kidney and epididymis. PLoS One 4:e4471. doi:10.1371/journal.pone.0004471

54. Wagner CA, Devuyst O, Bourgeois S, Mohebbi N (2009) Regulated acid-base transport in the collecting duct. Pflugers Arch 458:137-156. doi:10.1007/s00424-009-0657-z

55. Wagner CA, Finberg, K E, Stehberger, P A, Lifton, R P, Giebisch, G H, Aronson, P S, Geibel, J P (2002) Regulation of the expression of the Cl^-/anion exchanger pendrin in mouse kidney by acid-base status. Kidney Int 62:2109-2117

56. Wagner CA, Loffing-Cueni D, Yan Q, Schulz N, Fakitsas P, Carrel M, Wang T, Verrey F, Geibel JP, Giebisch G, Hebert SC, Loffing J (2008) Mouse model of type II Bartter's syndrome. II. Altered expression of renal sodium- and water-transporting proteins. Am J Physiol Renal Physiol 294:F1373-1380. doi:00613.2007 [pii]

10.1152/ajprenal.00613.2007

57. Wagner CA, Mohebbi N, Capasso G, Geibel JP (2011) The Anion Exchanger Pendrin (SLC26A4) and Renal Acid-base Homeostasis. Cell Physiol Biochem 28:497-504. doi:000335111 [pii]

10.1159/000335111

58. Wall SM (2016) The role of pendrin in blood pressure regulation. Am J Physiol Renal Physiol 310:F193-203. doi:ajprenal.00400.2015 [pii]

10.1152/ajprenal.00400.2015

59. Wall SM, Hassell, K A, Royaux, I E, Green, E D, Chang, J Y, Shipley, G L, Verlander J W (2002) Localization of Pendrin in Mouse Kidney. Am J Physiol Renal Physiol 284:F229-241

60. Wall SM, Kim YH, Stanley L, Glapion DM, Everett LA, Green ED, Verlander JW (2004) NaCl restriction upregulates renal Slc26a4 through subcellular redistribution: role in Cl- conservation. Hypertension 44:982-987

61. Wall SM, Lazo-Fernandez Y (2015) The role of pendrin in renal physiology. Annu Rev Physiol 77:363-378. doi:10.1146/annurev-physiol-021014-071854

62. Wehrli P, Loffing-Cueni D, Kaissling B, Loffing J (2007) Replication of segment-specific and intercalated cells in the mouse renal collecting system. Histochemistry and cell biology 127:389-398

63. Welsh-Bacic D, Nowik M, Kaissling B, Wagner CA (2011) Proliferation of acid-secretory cells in the kidney during adaptive remodelling of the collecting duct. PLoS One 6:e25240. doi:10.1371/journal.pone.0025240

PONE-D-11-12365 [pii]

64. Wen D, Ni L, You L, Zhang L, Gu Y, Hao CM, Chen J (2012) Upregulation of nestin in proximal tubules may participate in cell migration during renal repair. Am J Physiol Renal Physiol 303:F1534-1544. doi:ajprenal.00083.2012 [pii]

10.1152/ajprenal.00083.2012

65. Werth M, Schmidt-Ott KM, Leete T, Qiu A, Hinze C, Viltard M, Paragas N, Shawber CJ, Yu W, Lee P, Chen X, Sarkar A, Mu W, Rittenberg A, Lin CS, Kitajewski J, Al-Awqati Q, Barasch J (2017) Transcription factor TFCP2L1 patterns cells in the mouse kidney collecting ducts. Elife 6. doi:10.7554/eLife.24265

66. Werth M, Walentin K, Aue A, Schonheit J, Wuebken A, Pode-Shakked N, Vilianovitch L, Erdmann B, Dekel B, Bader M, Barasch J, Rosenbauer F, Luft FC, Schmidt-Ott KM (2010) The transcription factor grainyhead-like 2 regulates the molecular composition of the epithelial apical junctional complex. Development 137:3835-3845. doi:137/22/3835 [pii]

10.1242/dev.055483

67. Wu H, Chen L, Zhou Q, Zhang X, Berger S, Bi J, Lewis DE, Xia Y, Zhang W (2013) Aqp2-expressing cells give rise to renal intercalated cells. J Am Soc Nephrol 24:243-252. doi:10.1681/ASN.2012080866

68. Yamaguchi Y, Yonemura S, Takada S (2006) Grainyhead-related transcription factor is required for duct maturation in the salivary gland and the kidney of the mouse. Development 133:4737-4748. doi:dev.02658 [pii]

10.1242/dev.02658

Table 1

	AE1 pos total (%)	AE1 pos/ BrdU pos (%)	Pds pos total (%)	Pds pos/ BrdU neg (%)	AQP2 pos total (%)	AQP2 pos/ BrdU pos (%)	n cells (n mice)
Control 12 hrs	20.9 ± 0.8	0.7 ± 0.5	24.6 ± 0.9	0.1 ± 0.1	52.6 ± 1.0	1.0 ± 0.4	2917 (5)
$NaHCO_3$ 12 hrs	22.1 ± 0.8	0.1 ± 0.1	23.4 ± 1.1	0.1 ± 0.1	54.5 ± 0.8	0.8 ± 0.2	4262 (5)
NaCl 12 hrs	19.8 ± 0.7	0 ± 0	23.7 ± 0.8	0 ± 0	56.6 ± 0.8	0.8 ± 0.2	3380 (5)
Control 24 hrs	20.2 ± 0.7	0.1 ± 0.1	26.5 ± 1.0	0 ± 0	53.2 ± 0.9	1.4 ± 0.4	3454 (5)
$NaHCO_3$ 24 hrs	21.7 ± 0.9	0 ± 0	26.7 ± 1.1	0 ± 0	51.6 ± 1.0	0.7 ± 0.3	2335 (5)
NaCl 24 hrs	20.0 ± 1.0	0 ± 0	27.8 ± 1.1	0 ± 0	52.3 ± 1.0	1.1 ± 0.4	2677 (5)
Control 7 days	21.5 ± 0.8	0.1 ± 0.1	23.3 ± 1.1	0 ± 0	55.1 ± 1.1	0.2 ± 0.1	3256 (5)
$NaHCO_3$ 7 days	19.6 ± 0.6*	0 ± 0	25.3 ± 0.9*	0.1 ± 0.1	55.1 ± 0.8	1.7 ± 0.3*	5732 (5)
NaCl 7 days	22.7 ± 0.8	0 ± 0	22.5 ± 1.2	0.1 ± 0.1	54.8 ± 1.2	1.5 ± 0.3*	2383 (5)

Table 2

	AE1 pos total (%)	AE1 pos/ Ki67 pos (%)	Pds pos Total (%)	Pds pos/ Ki67 pos (%)	AQP2 pos total (%)	AQP2 pos/ Ki67 pos (%)	n cells (n mice)
Control 24 hrs	12.2 ± 0.7	1.4 ± 0.8	29.7 ± 1.1	0.0 ± 0.0	58.2 ± 1.2	4.1 ± 1.2	1824 (5)
$NaHCO_3$ 24 hrs	11.3 ± 0.8	0.4 ± 0.4	25.2 ± 2.1	0.0 ± 0.0	63.6 ± 2.0	9.5 ± 1.8*	972 (5)
NaCl 24 hrs	10.8 ± 1.0	4.8 ± 2.6	30.0 ± 1.7	0.5 ± 0.3	59.2 ± 1.8	3.1 ± 1.1	1045 (5)
Control 7 days	12.0 ± 1.0	1.7 ± 1.0	23.8 ± 1.5	1.3 ± 0.9	64.2 ± 1.3	3.3 ± 0.7	1463 (5)
$NaHCO_3$ 7 days	9.6 ± 0.5*	4.3 ± 1.7	25.4 ± 1.4	0.4 ± 0.3	65.0 ± 1.2	7.8 ± 0.9	1983 (5)
NaCl 7 days	13.7 ± 0.7	3.1 ± 1.3	24.0 ± 1.2	0.4 ± 0.4	62.4 ± 1.2	7.5 ± 1.0	1756 (5)

Figure 1

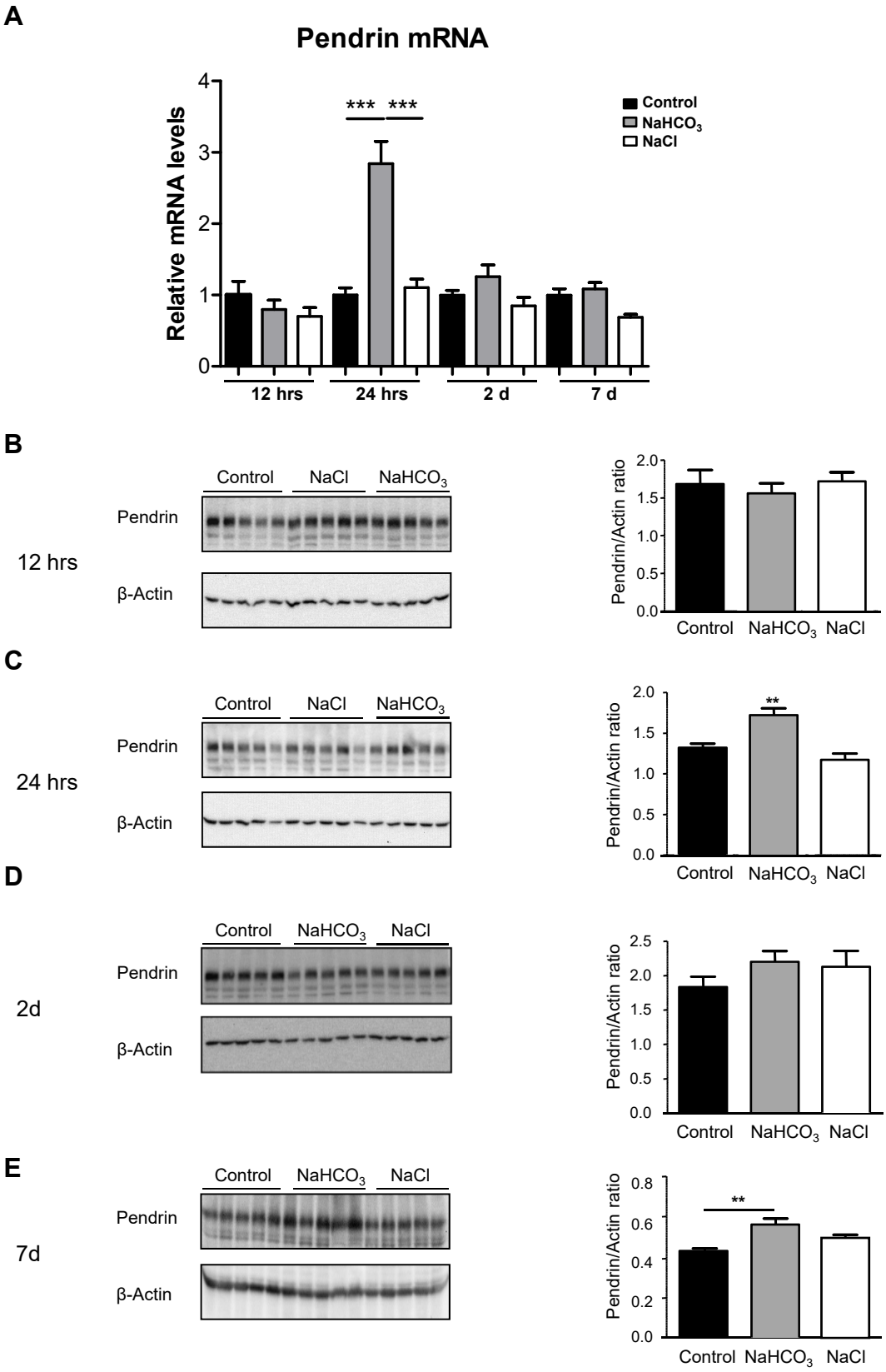
A
Pendrin mRNA
Relative mRNA levels
0
1
2
3
4
*** ***
Control
NaHCO3
NaCl
12 hrs
24 hrs
2 d
7 d
B
12 hrs
Control
NaCl
NaHCO3
Pendrin
β-Actin
Pendrin/Actin ratio
0.0
0.5
1.0
1.5
2.0
Control
NaHCO3
NaCl
C
24 hrs
Control
NaCl
NaHCO3
Pendrin
β-Actin
**
Pendrin/Actin ratio
0.0
0.5
1.0
1.5
2.0
Control
NaHCO3
NaCl
D
2d
Control
NaHCO3
NaCl
Pendrin
β-Actin
Pendrin/Actin ratio
0.0
0.5
1.0
1.5
2.0
2.5
Control
NaHCO3
NaCl
E
7d
Control
NaHCO3
NaCl
Pendrin
β-Actin
**
Pendrin/Actin ratio
0.0
0.2
0.4
0.6
0.8
Control
NaHCO3
NaCl

Figure 2

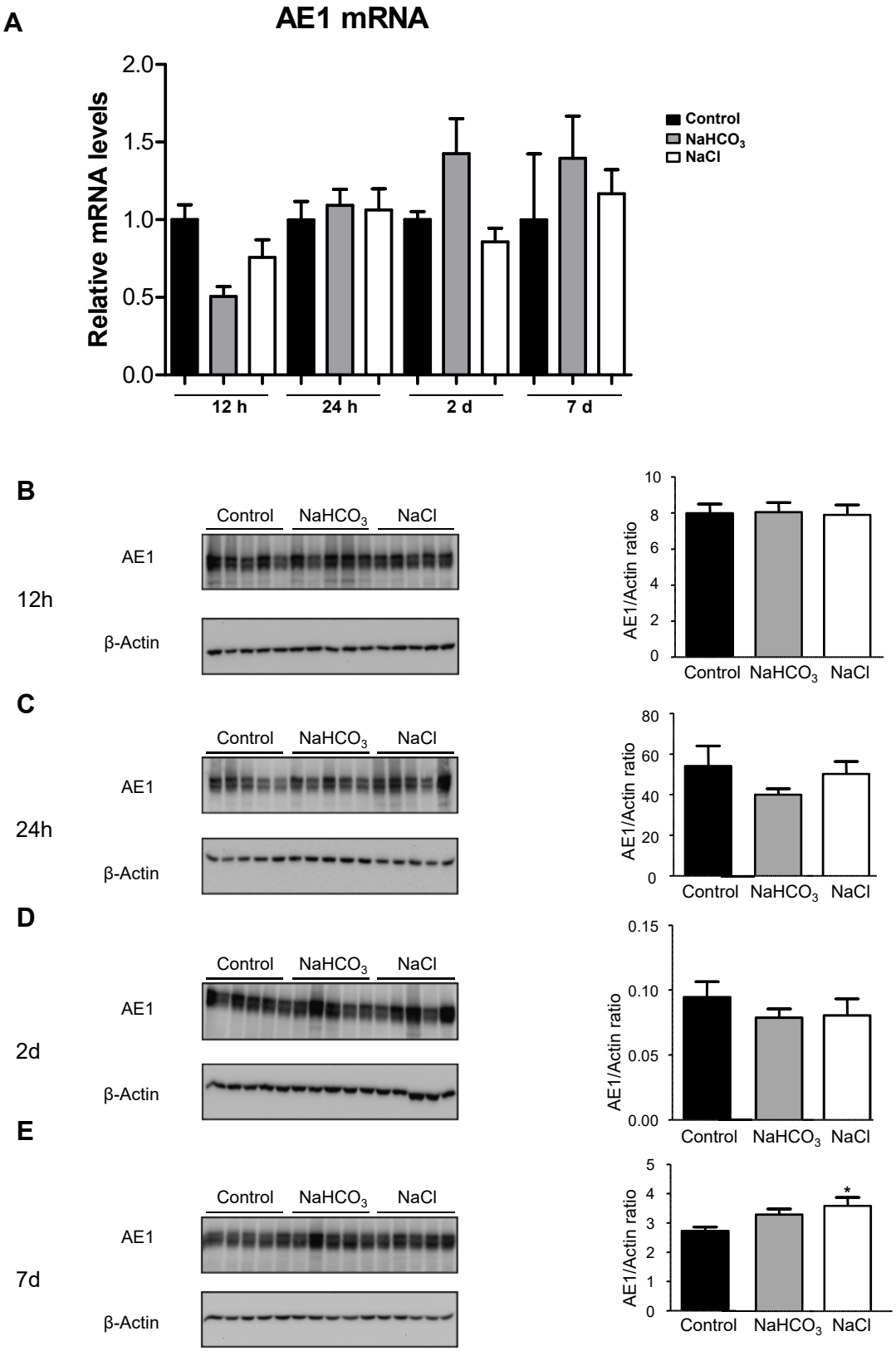
A
AE1 mRNA
Relative mRNA levels
2.0
1.5
1.0
0.5
0.0
12 h
24 h
2 d
7 d
Control
NaHCO3
NaCl
B
Control
NaHCO3
NaCl
AE1
12h
β-Actin
AE1/Actin ratio
10
8
6
4
2
0
C
24h
80
60
40
20
D
2d
0.15
0.10
0.05
0.00
E
7d
5
4
3
2
1
*

Figure 3

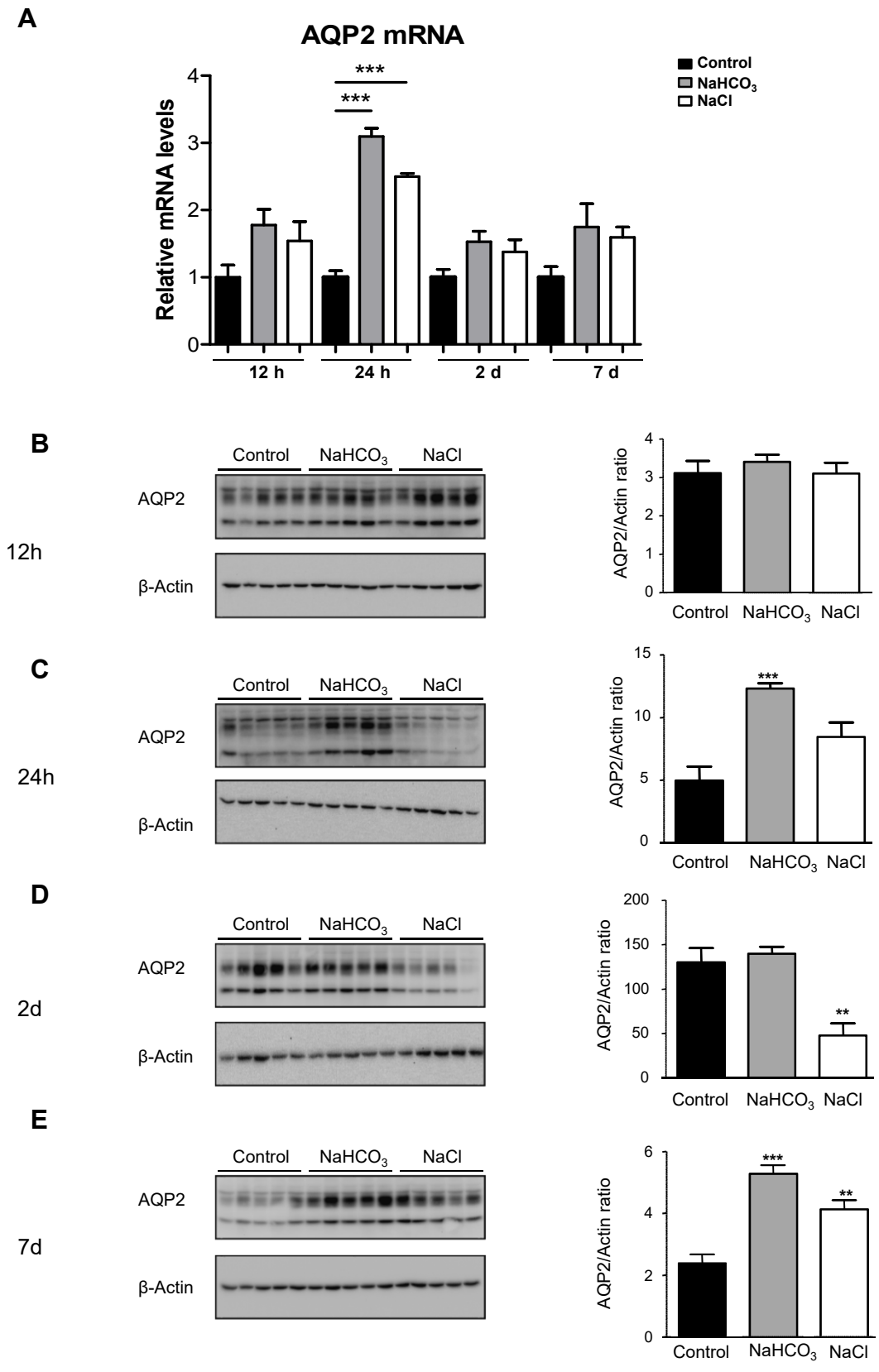
A
AQP2 mRNA
Relative mRNA levels
Control
NaHCO3
NaCl
***
***
12 h
24 h
2 d
7 d
B
12h
C
24h
D
2d
E
7d
Control
NaHCO3
NaCl
AQP2
β-Actin
AQP2/Actin ratio
**

Figure 4

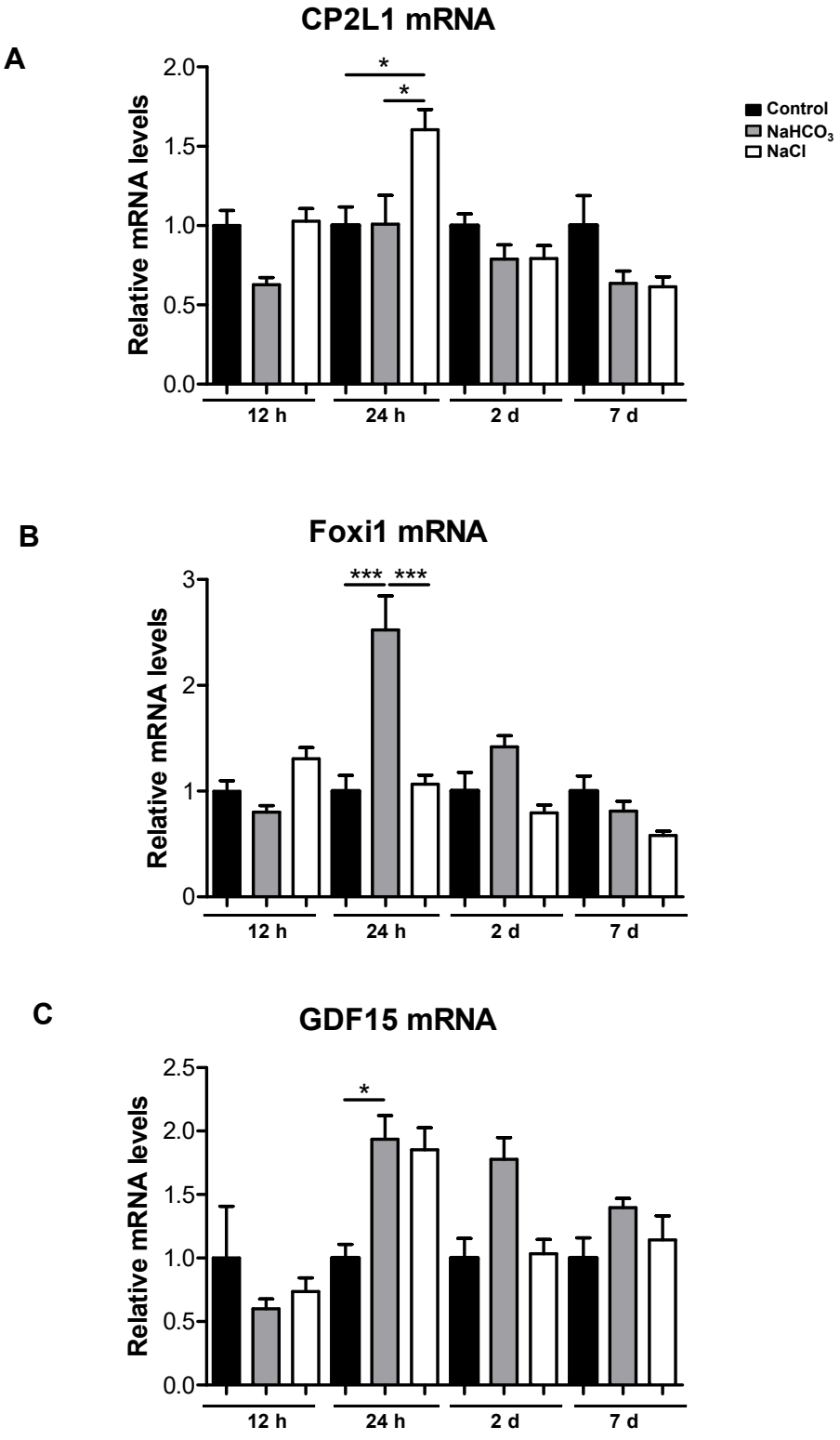
A
CP2L1 mRNA
Relative mRNA levels
2.0
1.5
1.0
0.5
0.0
*
*
Control
NaHCO3
NaCl
12 h
24 h
2 d
7 d
B
Foxi1 mRNA
Relative mRNA levels
3
2
1
0
***
***
12 h
24 h
2 d
7 d
C
GDF15 mRNA
Relative mRNA levels
2.5
2.0
1.5
1.0
0.5
0.0
*
12 h
24 h
2 d
7 d

Figure 5

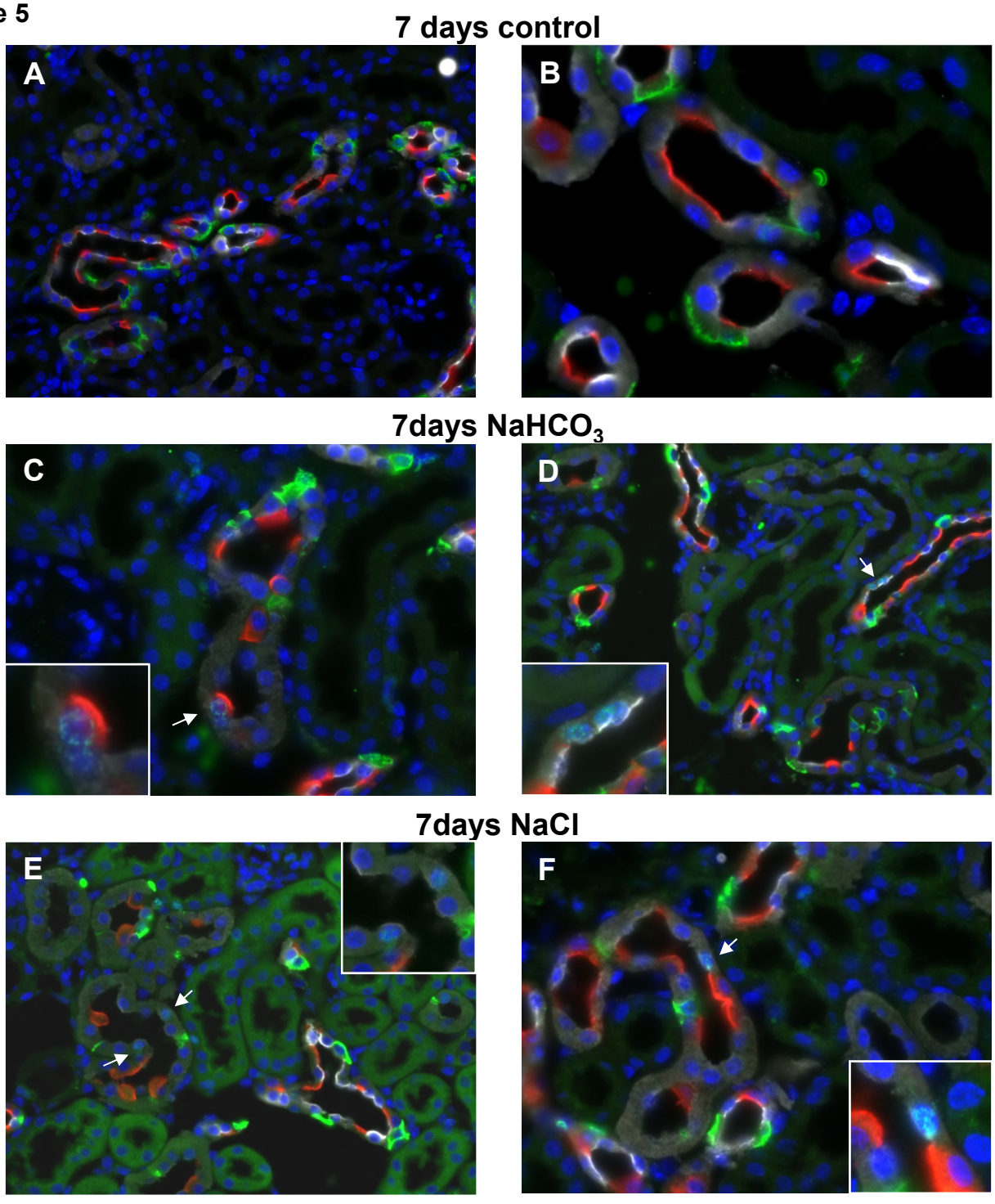

Pendrin red
AQP2 white
BrdU white
AE1 green
DAPI blue

Figure 6

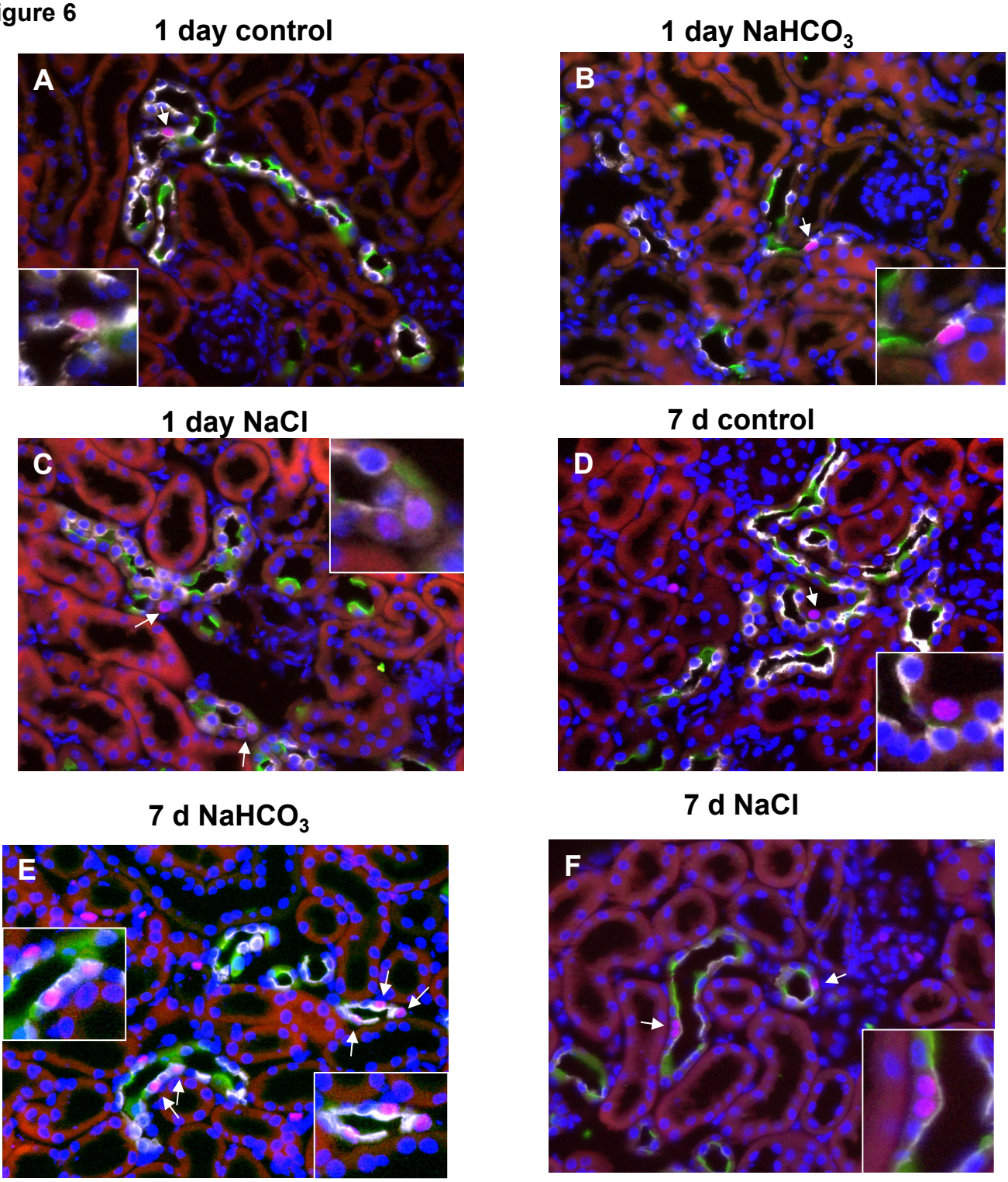

Ki67 red
AQP2 white
Pendrin green
DAPI blue